CORROSION RESISTANCE EVALUATION OF WELDED STAINLESS STEELS IN CONCRETE

M. J. Correia* — M. M. Salta* — I. T. E. Fonseca**

** LNEC, Laboratório Nacional de Engenharia Civil, DM, Av. do Brasil, 101, 1700-066 Lisboa, Portugal*
mjmcorreia@lnec.pt
msalta@lnec.pt

*** CCMM, FCUL, Faculdade de Ciências da Universidade de Lisboa, DQB, Edifício C8, 1749-016 Lisboa, Portugal*
itfonseca@fc.ul.pt

CORROSION RESISTANCE EVALUATION OF WELDED STAINLESS STEELS IN CONCRETE

M. J. Correia* — M. M. Salta* — I. T. E. Fonseca**

** LNEC, Laboratório Nacional de Engenharia Civil, DM, Av. do Brasil, 101, 1700-066 Lisboa, Portugal*
mjmcorreia@lnec.pt
msalta@lnec.pt

*** CCMM, FCUL, Faculdade de Ciências da Universidade de Lisboa, DQB, Edifício C8, 1749-016 Lisboa, Portugal*
itfonseca@fc.ul.pt

ABSTRACT. *The corrosion resistance of both welded and unwelded bars of Fe-Cr-Ni and Fe-Cr-Mn austenitic stainless steel alloys embedded in concrete was studied. Welded bars have been transiently either in an active or passive condition revealing its vulnerability to pitting corrosion, while unwelded bars have shown a stable passive state. The corrosion of the welded bars is mostly caused by the existence of weld surface defects, and by galvanic effects which are more considerable in the welded high manganese alloys.*

KEYWORDS: *Stainless steel reinforcement, new alloys, corrosion prevention, welding.*

1. Introduction

Reinforcement corrosion has become the most serious cause of premature deterioration of concrete structures. Thus, additional preventive measures are necessary to provide a long service life, especially for structures exposed to high environmental aggressiveness. From among the several preventive methods to counter reinforcement corrosion, the use of reinforcement materials more resistant to corrosion, such as stainless steel, has proven to be an effective technical solution (Nürnberger, 1996; CSTR 51, 1998). The success of this preventive measure is a consequence of the good corrosion resistance of stainless steel in alkaline mediums.

Comparatively with carbon steel, the main disadvantage is the higher initial cost of stainless steel. To overcome this drawback some of the latest research efforts have been undertaken for developing new less costly high manganese stainless steel alloys, with similar mechanical properties and with an equivalent corrosion resistance to those exhibited by conventional Fe-Cr-Ni alloys (HIPER, 2005).

Even though stainless steel has a high corrosion resistance in alkaline medium, it remains susceptible to localized corrosion in high corrosivity conditions. Environmental variables and material properties are critical conditioning factors of the stainless steel pitting corrosion resistance. So, the local microstructural and surface state modifications induced by welding can decrease the corrosion performance of stainless steel.

According to the literature, the corrosion resistance of stainless steel is highly affected by welding (Nürnberger, 1996, 2000, 2005; CSTR 51, 1998; COST 521, 2003; Bertolini et al., 2004) due to superficial mill scale and temper colours, regardless of the improvement accomplished by surface treatments.

Reviewing this subject gives obvious indications of welding drawbacks. Nevertheless, further research is essential to identify the main conditioning factors of the performance of welded areas, in support to specifications for stainless steel use in concrete and to the development of new alloys.

The corrosion resistance in concrete of welded bars of both new and conventional austenitic stainless steel alloys is assessed and compared with the behaviour of unwelded bars. The research is further extended through tests in solution to evaluate the effect, on corrosion resistance, of removing scale and superficial defects from the welded area.

2. Experimental

2.1 Electrode materials

Tests were performed on five austenitic stainless steel alloys - two Fe-Cr-Ni alloys (1.4301 and 1.4436 according to EN10088-1:2005; identified respectively as SS0 and SS4) and three recently developed high manganese alloys (SS1, SS2, and SS3). Table 1 indicates the chemical composition of the studied alloys.

Table 1. *Chemical composition of steel alloys (weight %).*

	C	Mn	Si	P	S	Cr	Ni	Mo	N	Cu	V
SS0	0.05	1.49	0.39	0.04	0.01	18.21	8.50	0.43	0.077	0.36	0.085
SS1	0.07	8.14	0.19	0.02	<0.001	16.52	0.22	<0.005	0.158	1.94	0.069
SS2	0.04	8.26	0.15	0.01	<0.001	16.50	1.23	1.93	0.290	2.06	0.072
SS3	0.04	11.30	0.39	0.02	<0.001	16.85	2.17	0.07	0.360	2.50	0.067
SS4	0.02	1.86	0.36	0.03	0.02	17.38	12.85	2.70	0.061	0.34	0.098

2.2 Metallography

The microstructures of both welded and unwelded areas in the tested sample bars were observed on an Olympus PMG3 metallographic microscope, after grinding, polishing with emery paper and diamond paste down to 1 μm, and appropriate etching. The stainless steel alloys were electrolytic etched with a 10% oxalic acid solution. The grain size and the inclusions content were respectively characterised by comparison (ASTM E 112-96) and method A (ASTM E 45-97).

2.3 Electrochemical measurements

The electrochemical experiments were performed with a PCI4/300 Gamry electrochemical system.

2.3.1 Electrochemical tests in concrete

Samples with an 8-cm length were cut from ribbed bars (ϕ 12 mm) of each stainless steel alloy (unwelded samples). Welded samples consist of two ribbed pieces of each alloy, with a 4-cm length, welded by arc welding with 1.4436 electrodes. Both welded and unwelded samples were brushed, cleaned and assembled to a mould to achieve a 10 mm concrete cover in concrete slabs (30x30x10 cm). However, the welded area, due to its irregular shape, has a minimum 6 mm concrete cover on some areas.

The embedded steel samples have been exposed periodically to a 3.5 % sodium chloride solution in alternated dry/immersion cycles, having been monitored since the 41st day of exposure beginning. The open circuit potential of each sample was monitored, relatively to an embedded activated titanium electrode (TiA), with an Hp 34970A data acquisition switch unit. These electrodes have shown a medium open circuit potential value of (-2±2)x10 mV relatively to saturated calomel electrode (SCE). For the other electrochemical tests, a stainless steel mesh and a SCE were respectively used as counter and reference electrodes. The polarisation resistance was done at 4.17×10^{-2} mV s^{-1} scan rate from -10 mV to +10 mV relatively to the open circuit potential (E_{OCP}). Impedance spectroscopy tests were carried out with 10 mV rms ac modulation at E_{OCP}, in a frequency range from 10^5 to 0.01 Hz.

2.3.2 Potentiodynamic tests in $Ca(OH)_2$ saturated solution

The electrochemical experiments were conducted on a three electrode electrochemical cell in a saturated $Ca(OH)_2$ solution (pH≈12.6) with 10% chloride, after stabilisation for 10 minutes in solution at room temperature. Disc shaped working electrodes (length = 2 mm; diameter = 10 mm) were prepared from ribbed bars, with lengths ranging from 2 to 5 mm, from both welded and unwelded samples. Prior to the experiments, each electrode was polished with emery paper and with diamond paste down to 0.25 μm. Platinum and SCE were respectively used as counter and reference electrodes. The anodic polarisation was done at 1 mV s^{-1} scan rate from -50 mV, relatively to the open circuit potential (OCP) towards the transpassivation (Et) or pitting potentials (Ep). The scanning was reversed or stopped when reaching 10 μA cm^{-2} of current density, respectively when transpassivation or pitting potentials were attained.

3. Results

3.1 Microstructural analysis

Figure 1 shows the cross section microstructure of each studied alloy and the microstructural changes in welded areas. All alloys show an austenitic matrix, and the high manganese alloys show also some local grain boundary carbide precipitates and small areas of ferrite. In particular, the SS2 alloy presents an uneven distribution of second phase particles, showing a clear reduction in their amount from the centre to the surface of the transversal section. All alloys present a low severity level of inclusions except SS3, which has a high content of thin type C inclusions.

The welded area consists of three distinct zones, in particular, fusion zone (FZ), heat affected zone (HAZ), and base metal. The microstructure of the FZ is austenite and vermicular ferrite. The HAZ shows specific microstructural changes, in particular in the austenitic grain size and in ferrite density, especially in the high manganese alloys. The increase in ferrite density is more marked in SS2 alloy. SS3 shows more defects and higher inclusions in the HAZ than in the base alloy.

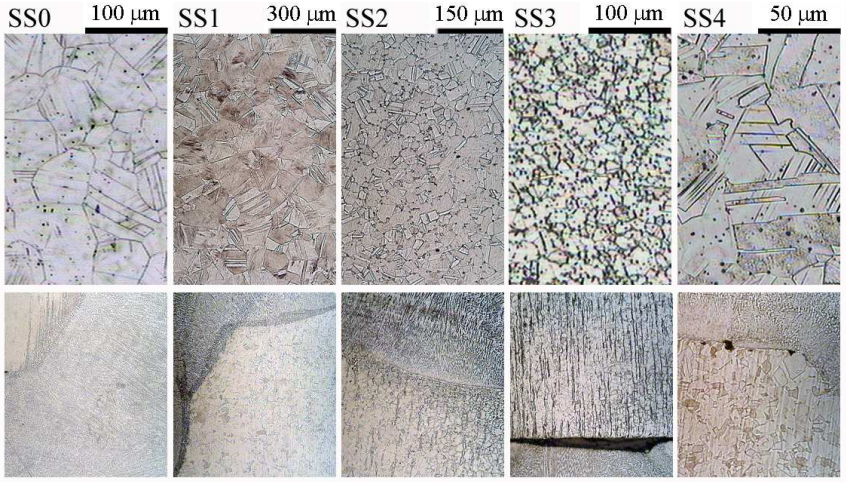

Figure 1. *Microstructure of both welded and unwelded samples of each alloy.*

3.2. Potential monitoring and electrochemical periodic results in concrete

Figure 2 shows the open circuit potential monitoring results of one unwelded sample of each stainless steel alloys.

Since the beginning of monitoring, a reduction (in cathodic direction) in the open circuit potential of SS1 and SS3 welded samples has been detected. The SS0, SS2, and SS4 welded samples show sharp cathodic potential decays associated to pitting events. The welded SS2 sample also exhibited longer propagation periods of pitting corrosion followed by repassivation.

The periodical electrochemical experiments give further support to the monitoring results. Polarization resistance results, indicated in figure 3, evidence the active corrosion of SS1 and SS3 and the periodical activation of SS2 and SS4. The open circuit potential and the polarization resistance mean values of SS1 and SS3 welded samples have been generally less than -0.3 V_{SCE} and 10^5 Ω cm^2, respectively. Pitting events were confirmed for SS0, SS2 and SS4 by a decrease in polarization resistance and potential. The high standard deviation associated with these results is caused by the distinct transient condition (active|passive) of each welded sample. Impedance spectroscopy shows the difference between active and passive state confirming the polarization resistance values, such as, for instance, the SS2 welded sample, of which the temporary depassivation is depicted in the diagrams of Figure 4.

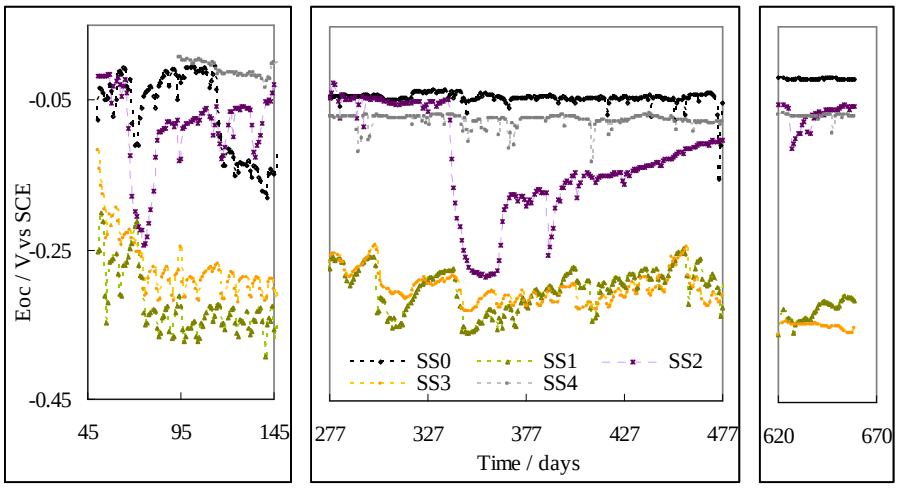

Figure 2. *Open circuit potential (E_{oc}) of stainless steel welded samples in concrete.*

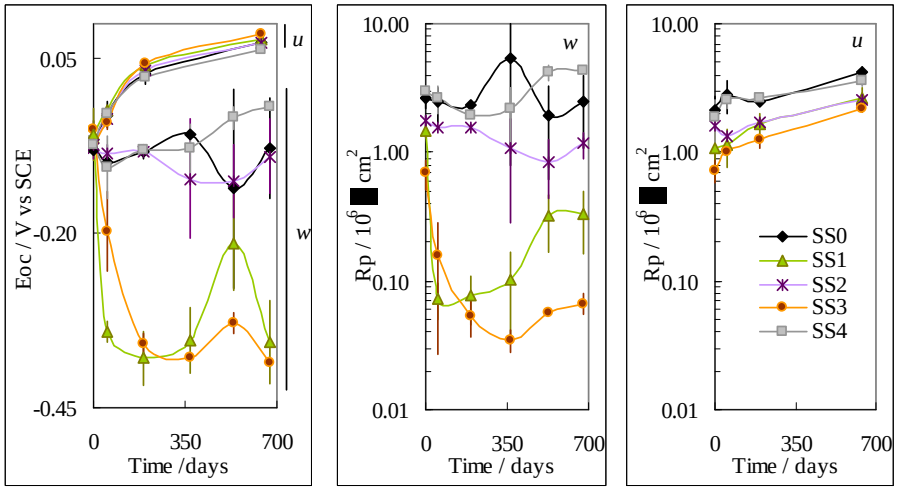

Figure 3. *Polarization resistance (R_p) and open circuit potential (E_{oc}) of stainless steel welded (w) and unwelded (u) samples in concrete.*

The unwelded stainless steel bar samples reveal a passive behaviour, by showing stable open circuit potential and polarization resistance values, respectively between 0.1 and -0.1 V_{SCE}, and higher than 10^6 Ω cm^2.

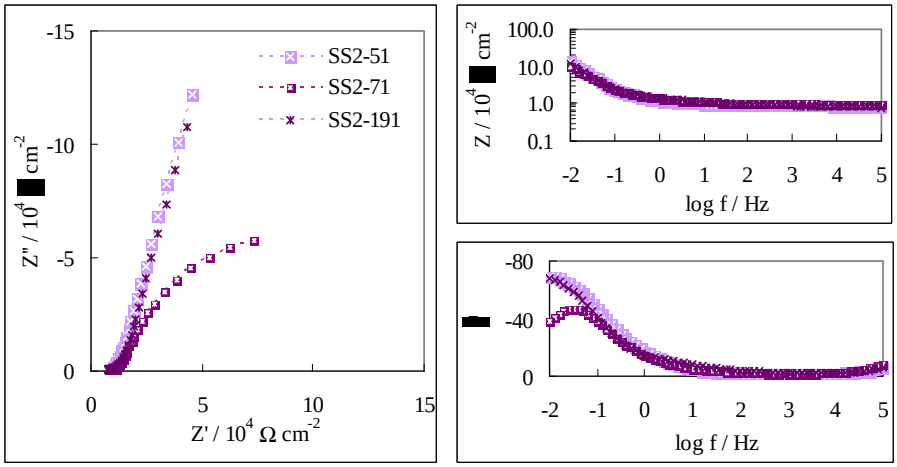

Figure 4. *Nyquist and Bode diagram of SS2 welded sample in concrete after 51, 71, and 191 days of exposure.*

3.3 Pitting corrosion resistance in $Ca(OH)_2$ saturated solution

In saturated $Ca(OH)_2$ solution with 10 % chloride addition, both welded and unwelded samples are susceptible to localized corrosion when the pitting potentials are exceeded (Table 2). These values are higher than 0.4 V_{SCE} except for SS3 welded sample, in consequence of its unavoidable superficial defects.

Table 2 – *Open circuit (E_{oc}) and pitting (E_p) potentials of stainless steel welded (w) and unwelded (u) samples in $Ca(OH)_2$ saturated solution with 10% Cl^-.*

	SS0		SS1		SS2		SS3		SS4	
	u	**w**	**u**	**w**	**u**	**w**	**u**	**w**	**u**	**w**
$\mathbf{E_{oc}}$	-0.45	-0.44	-0.41	-0.42	-0.42	-0.37	-0.39	-0.38	-0.43	-0.42
$\mathbf{E_p}$	0.49	0.46	0.47	0.47	0.49	0.41	0.40	0.13	0.48	0.45

4. Discussion

The alloys have shown a high corrosion resistance confirming previously reported results (García-Alonso et al., 2007).

The electrochemical results have shown the periodical activation of the welded samples, which is clearly evidenced by the potential transients obtained during monitoring. The lower corrosion resistance of welded samples is in accordance with the results from the literature (Nürnberger, 1996, 2000, 2005; CSTR 51, 1998; COST 521, 2003; Bertolini et al., 2004).

The critical chloride content associated with the depassivation of the welded alloys is 4.1% with respect to cement content, which is comparable to the 3.5 % value recommended in the literature (Bertolini et al., 2004).

The galvanic couple between base metal and filler metal, which can influence the corrosion process in the vicinity of the weld, is more significant in the high manganese alloys. After pitting nucleation, this galvanic effect may stabilise the pit propagation leading to longer lasting stable pitting corrosion events in Fe-Cr-Mn austenitic alloys. The superficial weld defects, which were not eliminated by the cleaning procedure, favoured the periodic activation of all welded alloys.

This hypothesis is confirmed by the similar corrosion resistance exhibited by most of the welded samples in solution after proper surface treatment. In $Ca(OH)_2$ saturated solution with 10 % chlorides, the welded samples are resistant to corrosion at open circuit conditions. Under analogous conditions of induced polarization both welded and unwelded samples have shown similar resistance to pitting corrosion proving that their performance is highly influenced by the surface state. SS3 was the only exception in consequence of the difficulties found in eliminating the surface irregularities in the HAZ.

5. Conclusions

The results obtained in this study confirm the critical influence of the surface condition on pitting corrosion. A proper surface treatment after welding and the avoidance of surface irregularities are extremely important procedures to prevent the pit nucleation. Another critical factor is a suitable selection of the welding electrode alloy thus preventing the major source of galvanic effects.

Especially SS1 and SS3 high manganese stainless steel welded samples have shown a stable propagation of pitting corrosion, being for that considered as the less resistant to corrosion. The galvanic effect, which is more significant in the high manganese alloys, may justify the distinct behaviour of welded Fe-Cr-Mn and Fe-Cr-Ni based alloys in concrete. However, the main factor explaining the difference between welded and unwelded samples is the surface state.

Fundação para a Ciência e Tecnologia (FCT), *Laboratório Nacional de Engenharia Civil* (LNEC), and DURATINET Project are gratefully acknowledged.

6. References

Bertolini L., Elsener B., Pedeferri P., Polder R., *Corrosion of steel in concrete – Prevention, Diagnosis, Repair*, WILEY-VCH, Weinheim, 2004.

Corrosion of steel in reinforced concrete structures, COST 521 Final Report, ed. by R. Cigna, C. Andrade, U. Nürnberger, R. Polder, R. Weydert and E. Seitz, 2003.

García-Alonso M. C., González J. A., Miranda J., Escudero M. L., Correia M. J., Salta M. M., and Bennani A., "Corrosion behaviour of innovative stainless steels in mortar", *Cement and Concrete Research*, 37, 2007, pp. 1562-1569.

García-Alonso M. C., Escudero M. L., Miranda J. M., Vega M. I., F. Capilla, Correia M. J., Salta M. M., Bennani A., and González J. A.: "Corrosion behaviour of new stainless steels reinforcing bars embedded in concrete", *Cement and Concrete Research*, 37, 2007, pp. 1463-1471.

Guidance on the use of stainless steel reinforcement, Concrete Society Technical Report 51, 1998.

Increased infrastructure reliability by developing a low cost and high performance stainless steel rebars, GDR1-2000-25601 from EC, HIPER Project final report, 2005.

Nürnberger U., *Stainless steel in concrete*, EFC-18, The Institute of Materials, London, 1996.

Nürnberger U., "Supplementary corrosion protection of reinforcing steel", *Otto-Graf-Journal*, 11, 2000, pp. 77-108.

Nürnberger U., "Stainless steel reinforcement – a survey", *Otto-Graf-Journal*, 16, 2005, pp. 111-138.